Analysis of the Low-Mass $K\pi\pi$ Enhancement*

B. Forman, N. M. Gelfand, P. Leary, F. Moser, A. Seidl,† and J. Wolfson
The Enrico Fermi Institute and Department of Physics, The University of Chicago, Chicago, Illinois 60637
(Received 2 November 1970; revised manuscript received 8 March 1971)

The reaction $K^+p \to K^+p\pi^+\pi^-$ at 4.3 BeV/c has been studied to investigate the nature of the low-mass $K\pi\pi$ enhancement. We find that the enhancement decays principally into $K^*(890)\pi$ with the $K^*(890)$ alignment the same as for the $K^*(890)$ from the final state $K^*(890)N^*(1236)$. We interpret the similar $K^*(890)$ decay distributions in the two distinct samples of events as further support for the hypothesis that the Q enhancement is due to a Deck-type mechanism.

I. INTRODUCTION

We have studied the broad low-mass $K\pi\pi$ enhancement (the Q) in an exposure of the MURA-ANL 30-in. liquid hydrogen bubble chamber to a 4.3-BeV/c K^+ beam. The properties of the Q region are already agreed upon: The dominant spin-parity is 1^+, the isotopic spin is $\frac{1}{2}$, and the principal decay is into $K^*(890)\pi$.[1] We find similar decay dis-

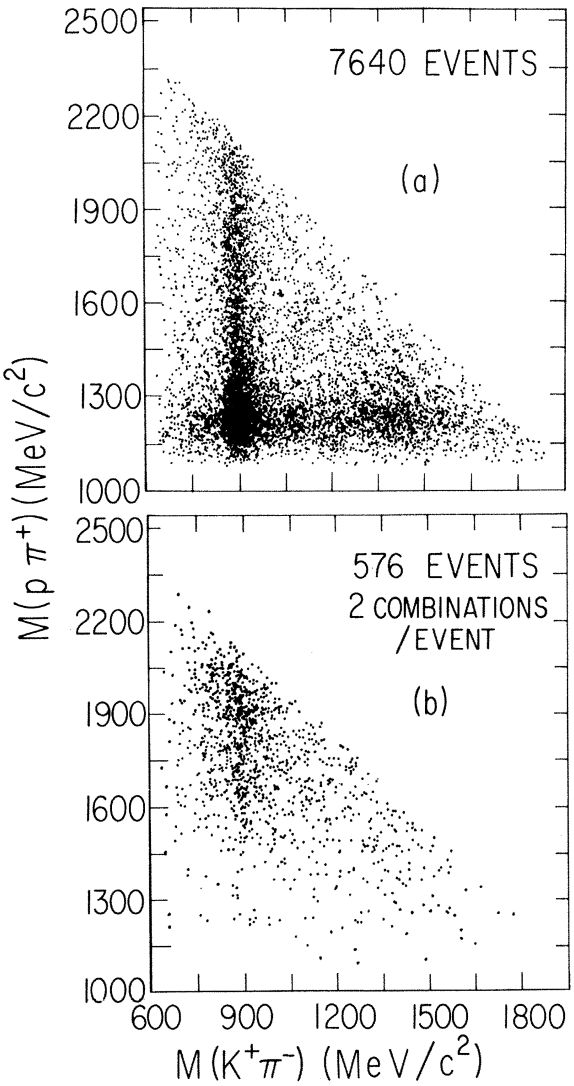

FIG. 1. Scatter plot of $M(p\pi^+)$ versus $M(K^+\pi^-)$ for (a) the unambiguous events; (b) the ambiguous events.

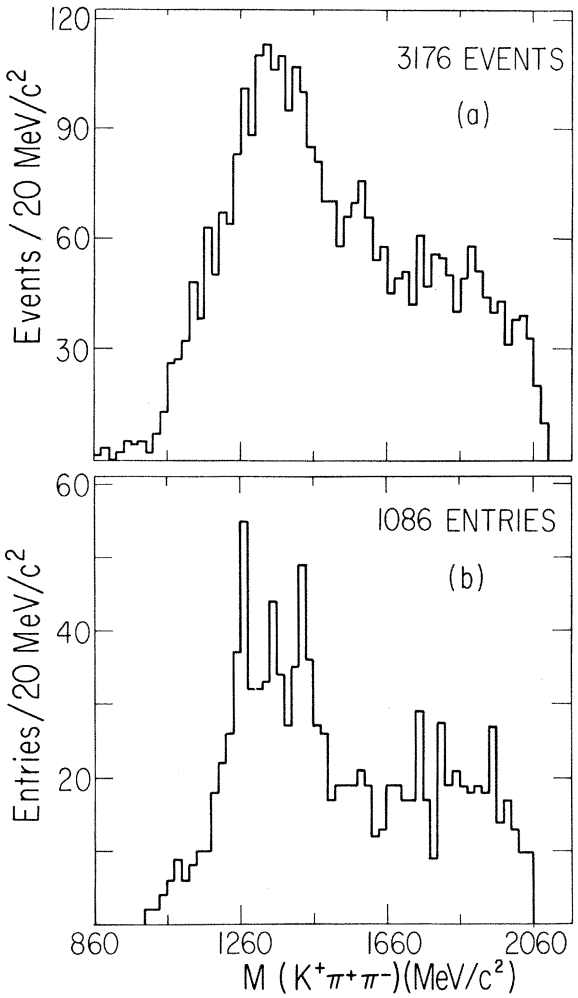

FIG. 2. $M(K^+\pi^+\pi^-)$ for the (a) unambiguous events for which $M(\pi^+p)$ is not in the N^* interval (1136–1336 MeV/c^2); (b) ambiguous events for the *hypotheses* for which $M(\pi^+p)$ is not in the N^* interval.

tributions for the $K^*(890)$ from the Q region and for the $K^*(890)$ which are produced with comparable cross section via one-pion exchange in the reaction $K^+p \to K^*(890)N^*(1236)$. This observation is new support for the suggestion of Deck[2] that threshold enhancements such as the Q are due to diffractive scattering of an exchanged pion from the target proton.

II. EVENT SELECTION

We have identified 8216 events of the reaction

$$K^+p \to K^+p\pi^+\pi^- . \quad (1)$$

(This sample constitutes approximately 60% of the total number of events expected in the exposure.) For 7640 of these events only one permutation of mass assignments among the tracks gives a fit which satisfies our four-constraint acceptance criteria: $\chi^2 < 20$ and all tracks having visual ionization estimates consistent with the fitted momenta and mass assignments. In the remaining 576 events the identification of one pair of positive tracks is ambiguous between two mass assignments. These ambiguous events have a distribution different from the unambiguous events on the $K^+\pi^-$ versus $p\pi^+$ scatter plot (Fig. 1). The unambiguous events are characterized by production of the $K^*(890)$ and the $N^*(1236)$ [Fig. 1(a)]. The ambiguous events show production only of the $K^*(890)$ [Fig. 1(b)]. The $K^+\pi^+\pi^-$ mass spectrum[3] (Fig. 2) is also different for the two sets of events. The ambiguous events have a larger fraction of events in the Q region than do the unambiguous events. We therefore feel it is necessary to include these ambiguous events in any analysis of the Q region.

The hypothesis selection criteria for ambiguous events are discussed in the Appendix. Here we summarize the criteria employed:

(a) The hypothesis with the higher χ^2 probability is chosen for all events with $K^+ \leftrightarrow p$ and $\pi^+ \leftrightarrow p$ ambiguities (104 events) and for those events with $K^+ \leftrightarrow \pi^+$ ambiguities for which the χ^2 probability ratio for the two hypotheses is greater than ten (98 events).

(b) If the ambiguity is a $K^+ \leftrightarrow \pi^+$ ambiguity and the χ^2 probability ratio is less than ten, production of $K^*(890)$ is used, if possible, as the basis for the

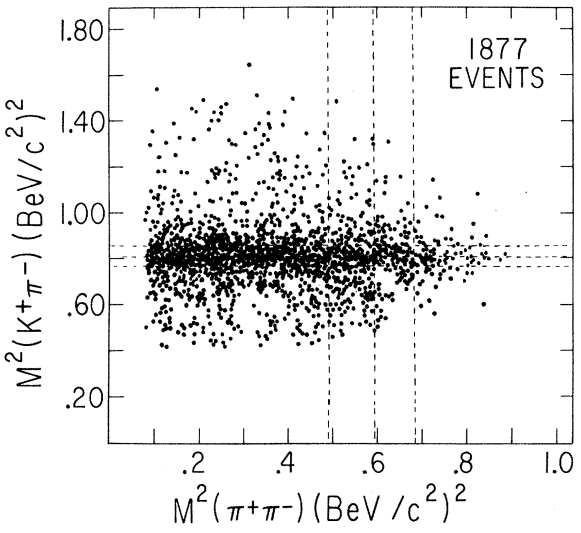

FIG. 3. Dalitz plot of $M^2(K^+\pi^-)$ versus $M^2(\pi^+\pi^-)$ for Q events with $M(K^+\pi^+\pi^-) < 1470$ MeV/c^2 and no (π^+p) combination in the N^* interval (1136–1336 MeV/c^2). The dashed lines indicate $K^*(890)$ and ρ regions.

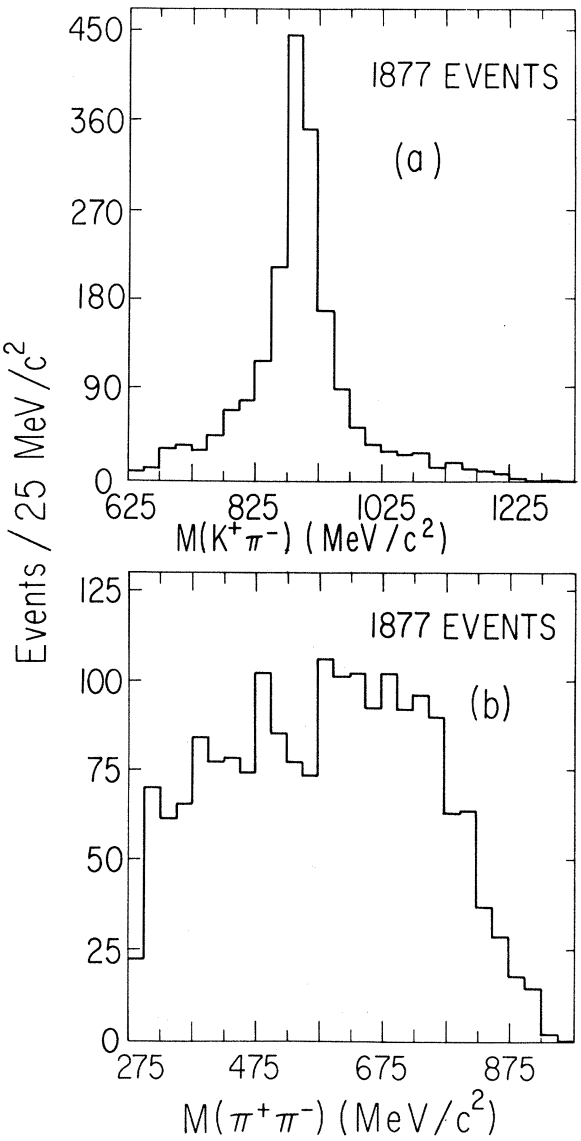

FIG. 4. Mass projections for the Q events with $M(K^+\pi^+\pi^-) < 1470$ MeV/c^2 and no (π^+p) combination in the N^* interval (1136–1336 MeV/c^2). (a) $M(K^+\pi^-)$; (b) $M(\pi^+\pi^-)$.

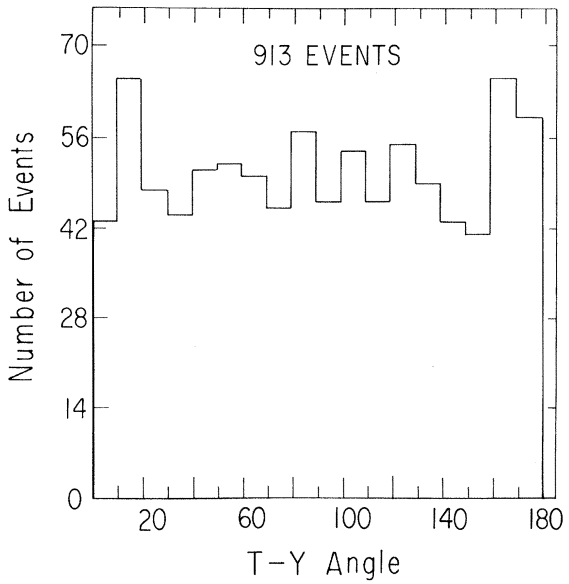

FIG. 5. Distribution of the Treiman-Yang angle in the $K^*(890)$ rest system for $M(K^+\pi^+\pi^-) < 1390$ MeV/c^2 and no N^* (1136–1336 MeV/c^2).

hypothesis selection (374 events).

The principal effect of this procedure appears in the $\pi^+\pi^-$ spectrum, as is discussed in the Appendix. These selection criteria do not involve the $K^+\pi^+\pi^-$ mass and we use the ambiguous events in our discussion of the Q.

III. THE Q ENHANCEMENT

The $K^+\pi^+\pi^-$ mass distribution, after we remove the $N^*(1236)$ events, shows a clear Q signal (Fig. 2). Peaks are seen in the $K\pi\pi$ mass spectrum at ~1260, ~1320, and ~1420 MeV/c^2. Without prejudicing a discussion of the existence of narrow $K\pi\pi$ resonances we note that the number of events in the peaks is small compared to the number in the broad background and proceed to analyze the entire region. Figure 3 is a Dalitz plot of $M^2(K^+\pi^-)$ versus $M^2(\pi^+\pi^-)$ for the Q events, those events with $K^+\pi^+\pi^-$ mass less than 1470 MeV/c^2. Both the Dalitz plot and the mass projection on the $K^+\pi^-$ axis (Fig. 4) show that the decay of the Q is dominated by the $K^*(890)$.

TABLE I. K^* decay angular distributions. $P(\mu) = 1 + A\mu + B\mu^2$, $\mu = \cos\theta_{KK}$.

	A	B
$K^*(890)N^*(1236)$ events	0.97 ± 0.12	4.02 ± 0.38
$K^*(890)$ events from Q decay[a]	0.63 ± 0.15	4.09 ± 0.55

[a] Using only the unambiguous events, we find $A = 0.51 \pm 0.16$ and $B = 4.18 \pm 0.61$.

By studying the decay of the K*(890) we learn about its mode of production. Figure 5 is the distribution of the Treiman-Yang angle in the $K^*(890)$ rest system for the Q events.[4] The isotropic distribution is consistent with $K^*(890)$ production via one-pion exchange. Figure 6(a) is the distribution of $\cos\theta_{KK}$, where θ_{KK} is the angle between the incident K^+ and the outgoing K^+ in the $K^*(890)$ rest system. The distribution is fitted to a power series in $\cos\theta_{KK}$ and the coefficients are shown in Table I.

As already noted, there is another distinct sample of $K^*(890)$: those seen in the reaction $K^+p \to K^*(890)N^*(1236)$ [Fig. 1(a)]. The $\cos\theta_{KK}$ distribution for these $K^*(890)$ is shown in Fig. 6(b) and

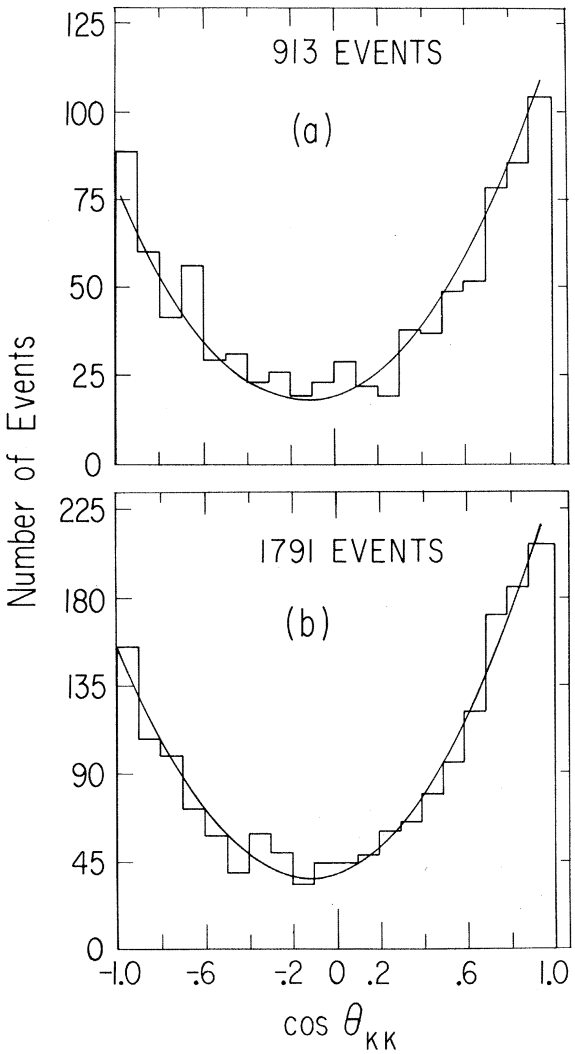

FIG. 6. Distribution of $\cos\theta_{KK}$ in the $K^*(890)$ rest system for (a) Q events with $M(K^+\pi^+\pi^-) < 1390$ MeV/c^2 and no $N^*(1136–1336$ MeV/c^2); (b) $K^*(890)$ $N^*(1236)$ events. The curves are from the fit to the K^*N^* events given in Table I, but normalized to the appropriate number of events.

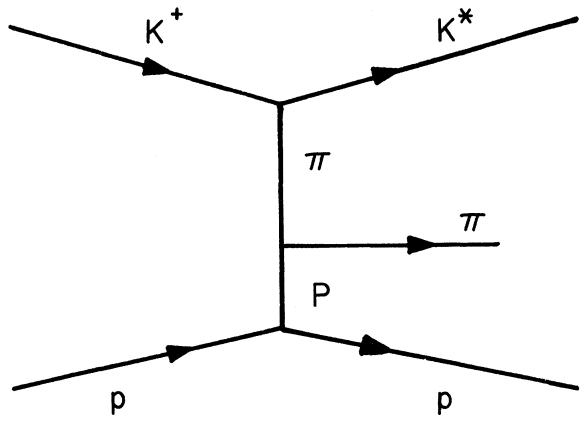

FIG. 7. Feynman diagram corresponding to the Deck model.

is fitted to a power series (Table I). This fit is normalized to the number of Q events – the events shown in Fig. 6(a) – and a χ^2 is computed to test whether the fit obtained for the $K^*(890)N^*(1236)$ events is consistent with the $\cos\theta_{KK}$ distribution of the $K^*(890)$ from Q decay. This χ^2 is 28 for 19 degrees of freedom, a 10% probability that the distributions are the same. The $K^*(890)$ from the $K^*(890)N^*(1236)$ events and from the Q events have the same decay angular distribution. Therefore it is reasonable to conclude that the production mechanism for both samples of $K^*(890)$ is the same. The dominant mechanism for $K^*(890)N^*(1236)$ production is one-pion exchange. On the basis of the distribution of the Treiman-Yang angle and the $\cos\theta_{KK}$ distribution, we conclude that the $K^*(890)$ associated with the Q region are also produced via one-pion exchange. This result does not depend on a particular formulation of a one-pion exchange model.

A possible explanation of the enhancement in the $K\pi\pi$ mass spectrum based on one-pion exchange has been advanced by Deck. A Reggeized version of Deck's model, due to Berger,[5] gives for the diagram in Fig. 7 the following matrix element:

$$|M|^2 \sim \lambda_0\, e^{a(M_{\pi p})t}(1+\alpha_\pi)^2(Q_{K^*\pi})^{2\alpha}(1-\cos\pi\alpha_\pi)^{-1},$$

where

TABLE II. Comparison of the experimental distributions to the Berger model.

Distribution	χ^2/degree of freedom
$K^*\pi$	92/28
K^*p	63/33
Treiman-Yang angle	47/17
t'_p	28/18
t'_{K^*}	452/9
$\cos\theta_{pp}$	14/10

$$\lambda_0 = [M_{\pi p}^2 - (M_\pi - M_p)^2][M_{\pi p}^2 - (M_\pi + M_p)^2],$$

$a(M_{\pi p})$ is the slope of the πp elastic differential cross section as a function of $M_{\pi p}$, t_p = momentum transfer to the proton,

$$\alpha_\pi = -(M_\pi^2 - t_{K^*})(1 + M_\pi^2 - t_{K^*})^{-1} = \alpha,$$

$$Q_{K^*\pi} = M_{K^*\pi}^2 - t_p - M_K^2 - (M_{K^*}^2 - M_K^2 - t_{K^*}) \times (t_p + t_{K^*} - M_\pi^2)(2t_{K^*})^{-1}.$$

Figures 8 and 9 are comparisons between the data and the predictions of the model. The agree-

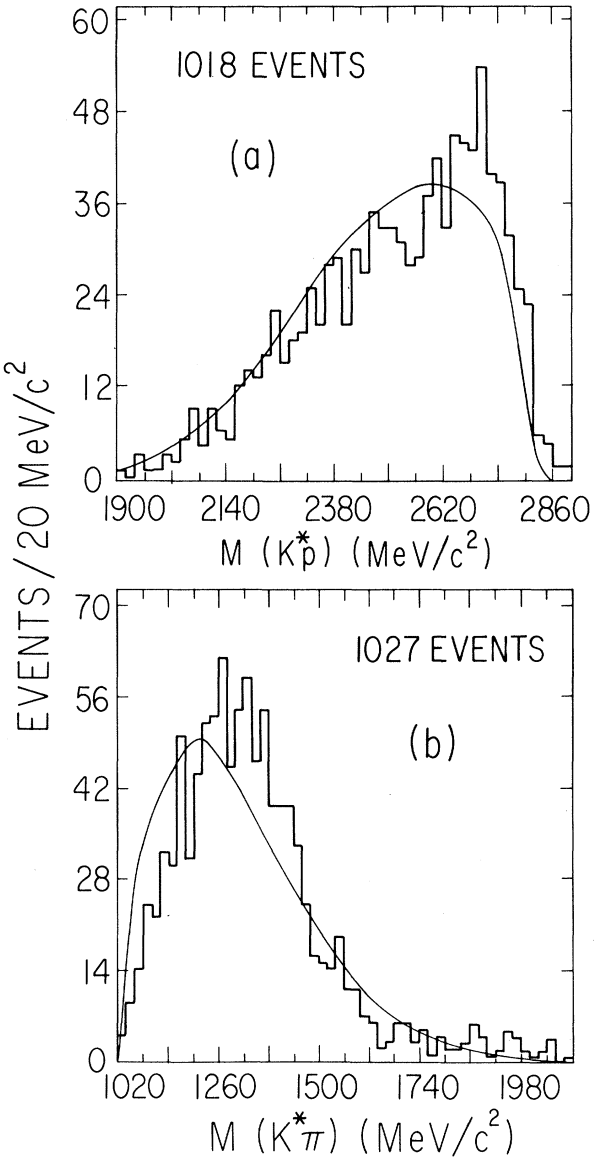

FIG. 8. Comparison of the Berger model with experimental distributions for (a) $K^*(890)p$ mass spectrum with $t'_p < 0.45$ BeV^2 and $t'_{K^*} < 0.6$ BeV^2; (b) $K^*(890)\pi^+$ mass spectrum with $t'_p < 0.45$ BeV^2 and $t'_{K^*} < 0.6$ BeV^2.

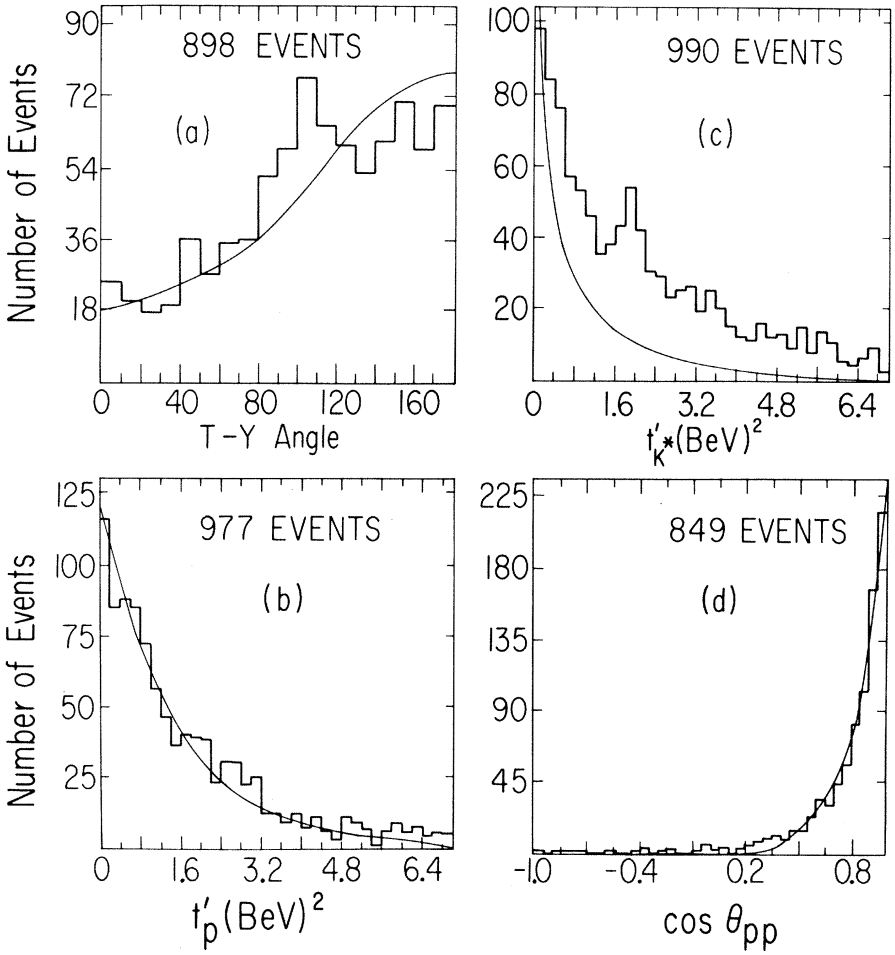

FIG. 9. Comparison of the Berger model with experimental distributions: (a) Treiman-Yang angle in the π^+p rest system for events with $t'_p < 0.45$ BeV^2, $t'_{K^*} < 0.6$ BeV^2, and $M(K^*\pi) < 1.47$ BeV/c^2; (b) t'_p for events with $M(K^*\pi) < 1.47$ BeV/c^2; (c) t'_{K^*} for events with $M(K^*\pi) < 1.47$ BeV/c^2; (d) $\cos\theta_{pp}$ in the π^+p rest system for events with $M(K^*\pi) < 1.47$ BeV/c^2, $t'_p < 0.45$ BeV^2, and $t'_{K^*} < 0.6$ BeV^2.

ment between the data and the model as measured by a χ^2 test (Table II), particularly for the t'_{K^*} distribution, cannot be considered good. However the model does reproduce the qualitative features of the data.

Without relying on the success of a specific model, we feel that the similarity in the $K^*(890)$ alignments is strong evidence for the importance of the diffractive one-pion exchange mechanism in Q production.

TABLE III. Ambiguous events.

		Events for which χ^2 probability ratio is >10	Events for which χ^2 probability ratio is <10
Hypothesis with the	higher χ^2 probability	IA	IIA
	lower χ^2 probability	IB Group I 98 events	IIB Group II 374 events

APPENDIX

The main source of ambiguous events in this exposure is the assignment of the K^+ and π^+ mass to a particular pair of tracks. The selection of the correct hypothesis in these ambiguous events of reaction (1) is particularly important in the study of the Q. The $K^+\pi^+\pi^-$ mass spectrum is not affected by the incorrect resolution of the ambiguity (being determined principally by the momentum of the unambiguously identified proton) but the $K^+\pi^-$ and $\pi^+\pi^-$ mass spectra can be very significantly distorted. The essential reason for this can be understood as follows. Imagine an event in which for a pair of the tracks the $K^+\pi^-$ mass is, as is very likely, ~890 MeV/c^2. If the K^+ is erroneously identified as a π^+, then the $\pi^+\pi^-$ effective mass of this same pair of tracks will be ~750 MeV/c^2. If

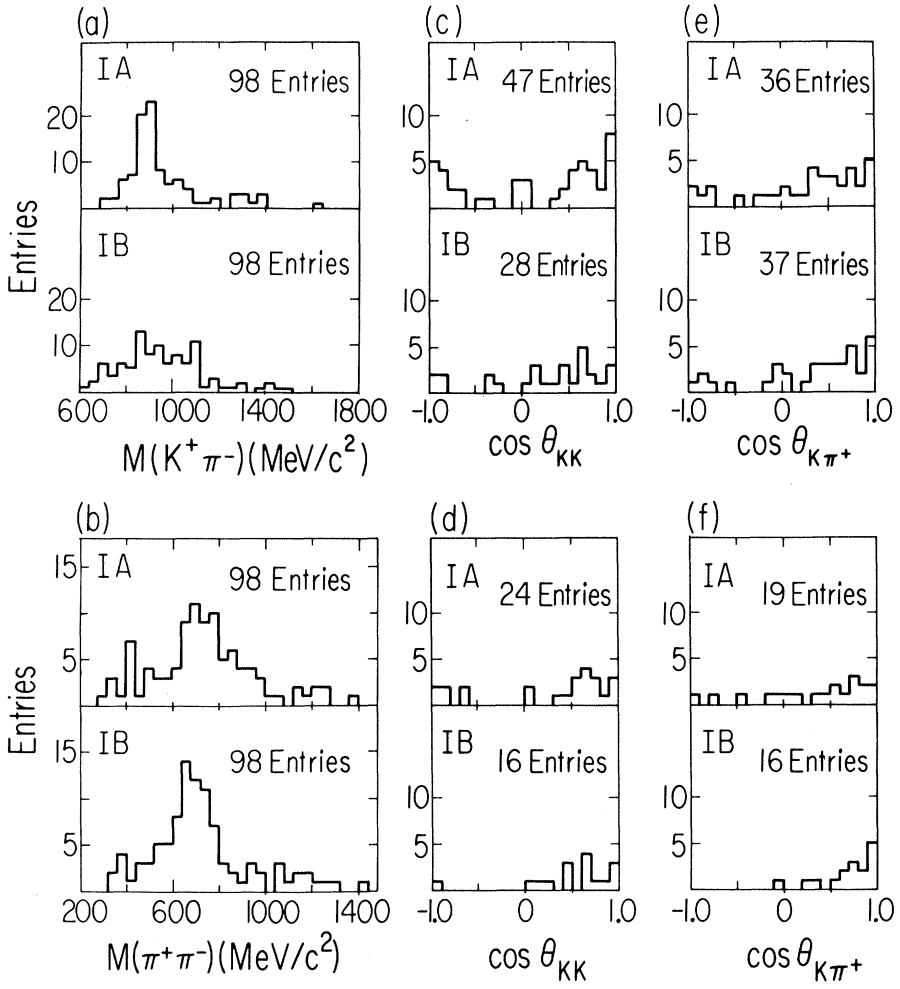

FIG. 10. Distributions for Group I events: (a) $M(K^+\pi^-)$ for hypotheses IA and IB; (b) $M(\pi^+\pi^-)$ for hypotheses IA and IB; (c) $\cos\theta_{KK}$ for IA hypotheses with $K^*(840\text{-}940\ \mathrm{MeV}/c^2)$ and for IB hypotheses with K^*; (d) $\cos\theta_{KK}$ for IA hypotheses with $M(K^*\pi) < 1390\ \mathrm{MeV}/c^2$ and for IB hypotheses with $M(K^*\pi) < 1390\ \mathrm{MeV}/c^2$; (e) $\cos\theta_{K\pi^+}$ for IA hypotheses with "ρ" $(675\text{–}825\ \mathrm{MeV}/c^2)$ and for IB hypotheses with "ρ"; (f) $\cos\theta_{K\pi^+}$ for IA hypotheses with $M(K\text{"}\rho\text{"}) < 1390\ \mathrm{MeV}/c^2$ and for IB hypotheses with $M(K\text{"}\rho\text{"}) < 1390\ \mathrm{MeV}/c^2$.

the $K^+\pi^-$ mass spectrum has a peak corresponding to the $K^*(890)$ and a substantial number of K^+ are identified as π^+, then there will be an apparent peak near the ρ mass in the "$\pi^+\pi^-$" mass spectrum. This erroneous peak can lead to serious errors in the analysis of the Q. We wish to show that misidentification occurs when χ^2 alone is used to resolve ambiguous events.

In the ambiguous events there are two acceptable hypotheses. One is certainly wrong; the other is presumably correct. We wish to devise some method by which we can, for each event, separate

TABLE IV. Comparison of distributions of hypotheses IIA to hypotheses IIB.

Variable	Probability that the IIA and IIB distributions are from the same sample
$K^+\pi^-$ mass	0.921
$\pi^+\pi^-$ mass	0.996
$\cos\theta_{KK}$, K^* events	0.843
$\cos\theta_{KK}$, K^* events, $M_{K^*\pi^+} < 1.39\ \mathrm{BeV}/c^2$	0.949
$\cos\theta_{K\pi}$, ρ events	0.952
$\cos\theta_{K\pi}$, ρ events, $M_{\rho K^+} < 1.39\ \mathrm{BeV}/c^2$	0.195

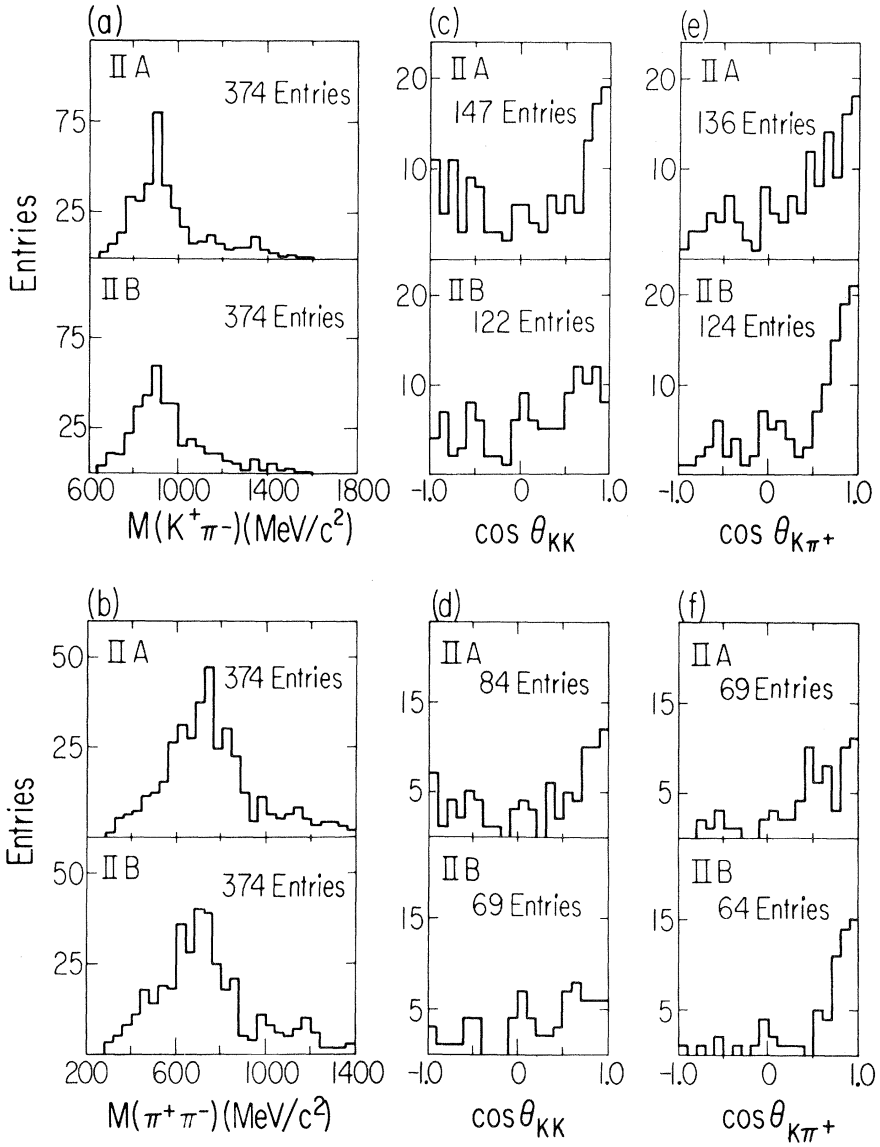

FIG. 11. Distributions for Group II events: (a) $M(K^+\pi^-)$ for hypotheses IIA and IIB; (b) $M(\pi^+\pi^-)$ for hypotheses IIA and IIB; (c) $\cos\theta_{KK}$ for IIA hypotheses with $K^*(840\text{–}940\ \mathrm{MeV}/c^2)$ and for IIB hypotheses with K^*; (d) $\cos\theta_{KK}$ for IIA hypotheses with $M(K^*\pi) < 1390\ \mathrm{MeV}/c^2$ and for IIB hypotheses with $M(K^*\pi) < 1390\ \mathrm{MeV}/c^2$; (e) $\cos\theta_{K\pi^+}$ for IIA hypotheses with "ρ" (675–825 MeV/c^2) and for IIB hypotheses with "ρ"; (f) $\cos\theta_{K\pi^+}$ for IIA hypotheses with $M(K$"ρ"$) < 1390\ \mathrm{MeV}/c^2$ and for IIB hypotheses with $M(K$"ρ"$) < 1390\ \mathrm{MeV}/c^2$.

the correct hypothesis from the incorrect one. If we are able to do so, we expect the distribution of some physically relevant variable to be different for the accepted hypotheses from that of the rejected hypotheses.[6]

We divide all the $K^+ \leftrightarrow \pi^+$ ambiguous events (there are two hypotheses per event) according to the scheme shown in Table III. For Group I events, those in which the χ^2 probability ratio between the two competing hypotheses is greater than 10, we believe that the probability ratio is a reliable discriminator. Group IA, the hypotheses with the higher χ^2 probability, then becomes the accepted sample. When we compare distributions for the hypotheses of IA (accepted) to IB (rejected), we observe obvious differences (Fig. 10).

However, when we compare distributions of IIA to IIB, we find similar distributions for the two subsamples (Fig. 11 and Table IV). The division based on χ^2 probability affects the Group II events in a way indistinguishable from a random selection criterion.

These distributions for the Group II events show a peak in the $\pi^+\pi^-$ mass spectrum near the ρ

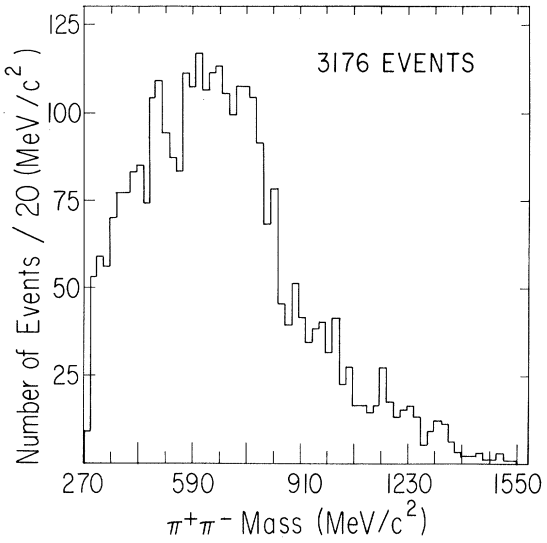

FIG. 12. $M(\pi^+\pi^-)$ for the unambiguous events for which $M(\pi^+p)$ is not in the N^* interval (1136–1336 MeV/c^2).

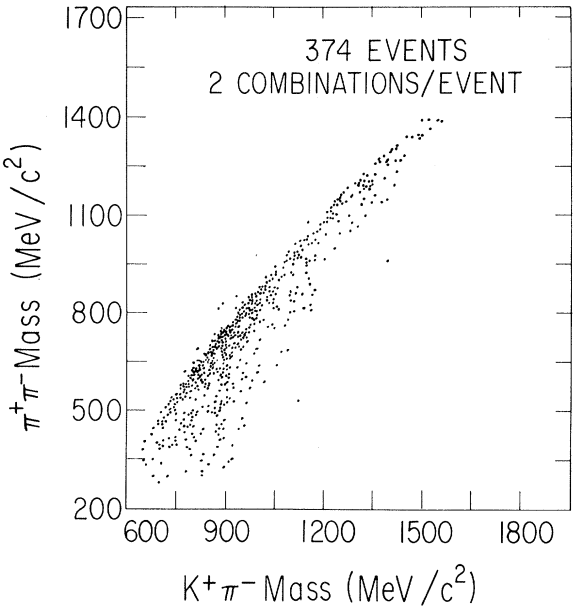

FIG. 13. Scatter plot for the Group II events of $M(K^+\pi^-)$ from one hypothesis versus $M(\pi^+\pi^-)$ from the alternate hypothesis. There are two entries per event.

[Fig. 11 (b)] which is not present in the unambiguous events (Fig. 12) or the Group I events [Fig. 10(b)]. Since the $\pi^+\pi^-$ peak in any one subsample (IIA or IIB) corresponds to the $K^*(890)$ peak in the alternate subsample (IIB or IIA), the $\pi^+\pi^-$ peak may stem from K^+'s misidentified as π^+'s (Fig. 13).

To decide if the peaks in the $\pi\pi$ mass spectra for the Group II events indicate ρ production or result from the misidentification of K^+ as π^+, we must resort to indirect arguments:

(a) The events in which we have the greatest confidence in our identification, the unambiguous events and the Group I events, show little evidence for a ρ.

(b) Even in the $K^+\pi^-$ mass spectrum of the IIB subsample, we find a prominent peak at ~895 MeV/c^2 in agreement with the accepted value of the $K^*(890)$ mass. However, the peak in the $\pi^+\pi^-$ mass spectrum for the IIA hypotheses is at ~700 MeV/c^2, rather far from the accepted value for the ρ mass [Figs. 11(a) and 11(b)].

(c) The χ^2 probability criterion for the Group II events does not divide the hypotheses into subsamples for which we observe significant differences.

In view of these arguments we do not feel that a χ^2 probability criterion leads to a dependable method of selecting between hypotheses for Group II

TABLE V. Comparison of accepted and rejected hypotheses: Group I events to Group II events.

Variable	Probability[a]
$K^+\pi^-$ mass – selected hypotheses for Groups I and II	0.03
$K^+\pi^-$ mass – rejected hypotheses for Groups I and II	0.16
$\pi^+\pi^-$ mass – selected hypotheses	0.02
$\pi^+\pi^-$ mass – rejected hypotheses	0.60
$\cos\theta_{KK}$, K^* events – selected hypotheses	0.26
$\cos\theta_{KK}$, K^* events – rejected hypotheses	0.68
$\cos\theta_{KK}$, K^* events, $M_{K^*\pi} < 1.39$ BeV/c^2 – selected hypotheses	0.09
$\cos\theta_{KK}$, K^* events, $M_{K^*\pi} < 1.39$ BeV/c^2 – rejected hypotheses	0.70
$\cos\theta_{K\pi}$, ρ events – selected hypotheses	0.42
$\cos\theta_{K\pi}$, ρ events – rejected hypotheses	0.16
$\cos\theta_{K\pi}$, ρ events, $M_{K\rho} < 1.39$ BeV/c^2 – selected hypotheses	0.65
$\cos\theta_{K\pi}$, ρ events, $M_{K\rho} < 1.39$ BeV/c^2 – rejected hypotheses	0.01

[a] Probability that the distributions for the accepted hypotheses of Group I and Group II are the same and the distributions for the rejected hypotheses of Group I and Group II are the same.

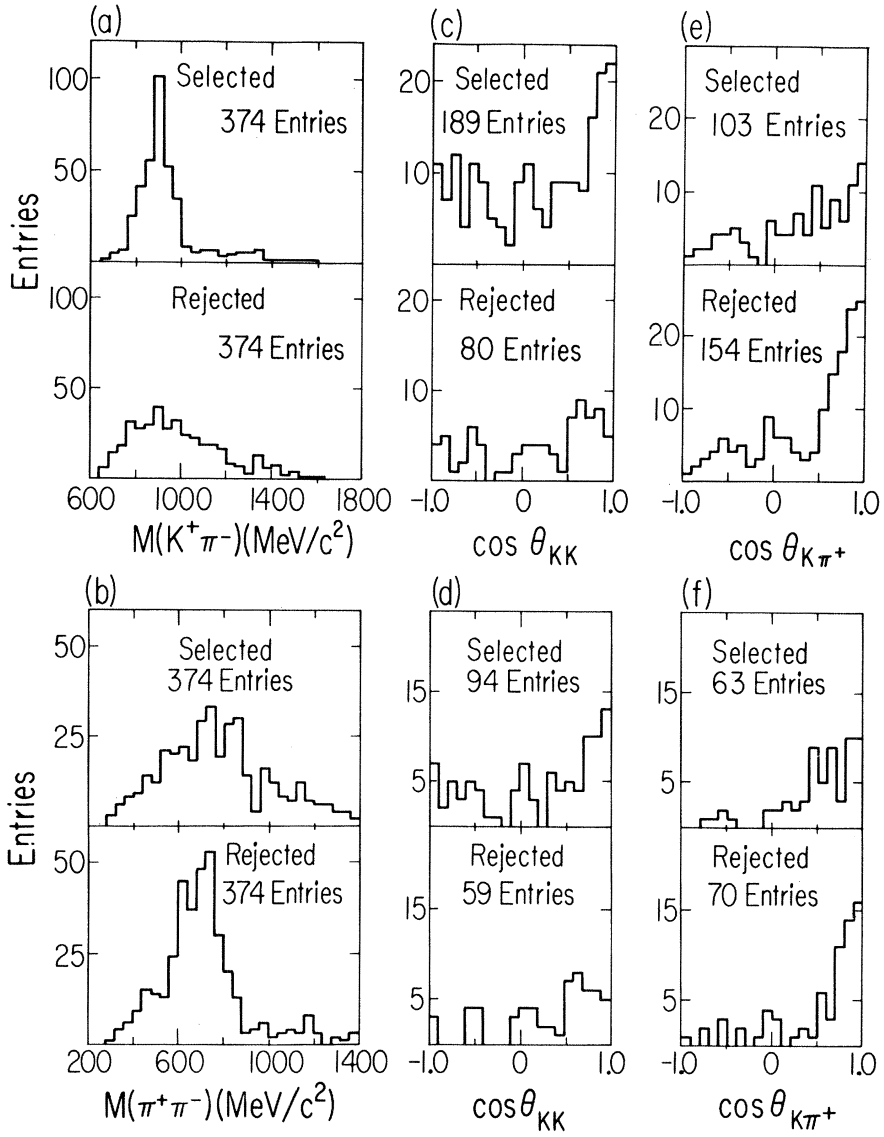

FIG. 14. Distributions for the selected and rejected hypotheses for the Group II events: (a) $M(K^+\pi^-)$ for the selected and rejected hypotheses; (b) $M(\pi^+\pi^-)$ for the selected and rejected hypotheses; (c) $\cos\theta_{KK}$ for the selected hypotheses with $K^*(840\text{–}940\ \mathrm{MeV}/c^2)$ and for the rejected hypotheses with K^*; (d) $\cos\theta_{KK}$ for the selected hypotheses with $M(K^*\pi) < 1390\ \mathrm{MeV}/c^2$ and for the rejected hypotheses with $M(K^*\pi) < 1390\ \mathrm{MeV}/c^2$; (e) $\cos\theta_{K\pi^+}$ for the selected hypotheses with "ρ" (675–825 MeV/c^2) and for the rejected hypotheses with "ρ"; (f) $\cos\theta_{K\pi^+}$ for the selected hypotheses with $M(K$"ρ"$) < 1390\ \mathrm{MeV}/c^2$ and for the rejected hypotheses with $M(K$"ρ"$) < 1390\ \mathrm{MeV}/c^2$.

events.

To resolve the ambiguity for Group II events, we make use of the fact that the narrow $K^*(890)$ dominates all the $K^+\pi^-$ spectra. We select one hypothesis on the basis of the strong $K^*(890)$ production observed in this final state. If only one of the two ambiguous hypotheses has a $K^+\pi^-$ mass between 790 MeV/c^2 and 990 MeV/c^2, that hypothesis is chosen. This criterion removes the ambiguity in 109 of the 374 Group II events. For the remaining 265 events of this group, we resort to choosing the hypothesis with the higher χ^2 probability to resolve the ambiguity[7]; we accept the IIA hypotheses for those events in which the K^* selection method cannot be applied. The distributions for all 374 ambiguous events of Group II, but with the ambiguities now resolved, if possible, with the criterion of $K^*(890)$ production, are shown in Fig. 14. With this choice of hypothesis there is no "ρ" peak in the $\pi^+\pi^-$ mass distribution. This is partly due to the selection criteria but the similarity between the distributions shown in Fig. 14 to those of Group I shown in Fig. 10 (Table V) suggests that the criteria are valid.

*Work supported in part by the National Science Foundation under Grant No. NSF GP 14521.

†E. I. DuPont Fellow, 1969–70.

[1]T. P. Wangler *et al.*, Phys. Letters 9, 71 (1964); R. Armenteros *et al.*, *ibid.* 9, 207 (1964); D. H. Miller *et al.*, *ibid.* 15, 74 (1965); S. P. Almeida *et al.*, *ibid.* 16, 184 (1965); A. R. Erwin *et al.*, Nucl. Phys. B9, 364 (1966); J. Bartsch *et al.*, Phys. Letters 22, 357 (1966); J. M. Bishop *et al.*, Phys. Rev. Letters 16, 1069 (1966); B. C. Shen *et al.*, *ibid.* 17, 726 (1966); W. de Baere *et al.*, Nuovo Cimento 49A, 373 (1967); G. Bassompierre *et al.*, Phys. Letters 26B, 30 (1967); J. C. Berlinghieri *et al.*, Phys. Rev. Letters 18, 1087 (1967); D. J. Crennell *et al.*, *ibid.* 19, 44 (1967); P. J. Dornan *et al.*, *ibid.* 19, 271 (1967); G. Goldhaber *et al.*, *ibid.* 19, 972 (1967); J. Bartsch *et al.*, Nucl. Phys. B8, 9 (1968); C. Y. Chien *et al.*, Phys. Letters 28B, 143 (1968); F. Schweingruber *et al.*, Phys. Rev. 166, 1317 (1968); J. C. Park *et al.*, *ibid.* 174, 2165 (1968); J. C. Park *et al.*, Phys. Rev. Letters 20, 171 (1968); D. Denegri *et al.*, *ibid.* 20, 1194 (1968); F. Bomse *et al.*, *ibid.* 20, 1519 (1968); J. M. Bishop *et al.*, Nucl. Phys. B9, 403 (1969); A. Astier *et al.*, *ibid.* B10, 65 (1969); G. Alexander *et al.*, *ibid.* B13, 503 (1969); D. C. Colley *et al.*, Nuovo Cimento 59A, 519 (1969); B. Werner *et al.*, Phys. Rev. 188, 2023 (1969); J. Andrews *et al.*, Phys. Rev. Letters 22, 731 (1969); Hsieh Jen-Shu *et al.*, Nucl. Phys. B18, 17 (1970); M. S. Farber *et al.*, Phys. Rev. D 1, 78 (1970).

[2]R. T. Deck, Phys. Rev. Letters 13, 169 (1964).

[3]Although the Q enhancement is clearly present before any $N^*(1236)$ cuts are imposed on the data, we have chosen to show and to study the $K\pi\pi$ spectrum after eliminating those events in the N^* interval 1136 MeV/$c^2 \leq M(\pi^+p) \leq 1336$ MeV/c^2. The $K^*(890)$ was defined as 840 MeV/$c^2 \leq M(K^+\pi^-) \leq 940$ MeV/c^2. The ρ region was defined as 675 MeV/$c^2 \leq M(\pi^+\pi^-) \leq 825$ MeV/c^2.

[4]In this study of the $K^*(890)$ decay the $K^+\pi^+\pi^-$ mass was required to be less than 1390 MeV/c^2 to reduce the contribution of the $K^*(1420)$ decay into $K^*(890)\pi$.

[5]E. L. Berger, Phys. Rev. 166, 1525 (1968).

[6]It is easy to believe that an assignment based on meaningless criteria, e.g., the frame number, will produce identical distributions for the accepted and rejected hypotheses. The converse need not be true. For a given variable, such as the laboratory momentum, both the correct and incorrect hypotheses may produce identical distributions. It would be surprising if this were true for the distributions in all variables.

[7]There are 80 events in Group II for which both hypotheses have the $K^+\pi^-$ mass combination in the $K^*(890)$ mass region and 185 events without a $K^*(890)$ in either hypothesis.

PHYSICAL REVIEW D VOLUME 3, NUMBER 11 JUNE 1971

π^-p Elastic Scattering in the c. m. Energy Range 1400–2000 MeV*

A. D. Brody,† R. J. Cashmore, A. Kernan,‡ D. W. G. S. Leith, B. S. Levi, and B. C. Shen‡
Stanford Linear Accelerator Center, Stanford University, Stanford, California 94305

and

J. P. Berge,§ D. J. Herndon, R. Longacre, L. R. Price,‖ A. H. Rosenfeld, and P. Söding**
Lawrence Radiation Laboratory, University of California, Berkeley, California 94720

(Received 7 December 1970)

Total and differential cross sections for π^-p elastic scattering are presented at 35 energies between 1400 and 2000 MeV.

I. INTRODUCTION

In recent years a large amount of data has been accumulated on the elastic and charge-exchange channels of πN scattering. Several extensive phase-shift analyses[1-7] performed on these data have uncovered much of the complicated resonance structure up to energies of 2000 MeV. The data and phase-shift results have been summarized by a number of authors.[8-11] Resonance parameters from some of the recent analyses are listed in Table I.[12] Despite good qualitative agreements, quantitative discrepancies still exist among the various solutions. These discrepancies exist in part because of the multidimensional parameter space explored and the different methods used, because of fluctuations between different experimental measurements, and finally, because the elastic data used are fairly insensitive to partial waves of low elasticity. Thus, the motivation for the present experiment was to fill the need for direct measurement of the inelastic channels. The systematic and rather complete set of measurements of the elastic channels, described in this paper, came as a by-product of this inelastic study.

We present below the first part of the results of a study of elastic and inelastic π^-p scattering at 35 momenta between 550 and 1600 MeV/c. Figure 1 illustrates the scope of the experiment. At each